

Dynamics of flexible tower-blade and rigid nacelle system: dynamic instability due to their interactions in wind turbine

Namcheol Kang, Sung Chul Park, Junhong Park and Satya N Atluri
Journal of Vibration and Control published online 14 May 2014
DOI: 10.1177/1077546314532119

The online version of this article can be found at:
<http://jvc.sagepub.com/content/early/2014/05/14/1077546314532119>

Published by:



<http://www.sagepublications.com>

Additional services and information for *Journal of Vibration and Control* can be found at:

Email Alerts: <http://jvc.sagepub.com/cgi/alerts>

Subscriptions: <http://jvc.sagepub.com/subscriptions>

Reprints: <http://www.sagepub.com/journalsReprints.nav>

Permissions: <http://www.sagepub.com/journalsPermissions.nav>


Citations: <http://jvc.sagepub.com/content/early/2014/05/14/1077546314532119.refs.html>

>> [OnlineFirst Version of Record](#) - May 14, 2014

[What is This?](#)

Dynamics of flexible tower-blade and rigid nacelle system: dynamic instability due to their interactions in wind turbine

Namcheol Kang¹, Sung Chul Park², Junhong Park³ and Satya N Atluri⁴

Journal of Vibration and Control
1-11
© The Author(s) 2014
Reprints and permissions:
sagepub.co.uk/journalsPermissions.nav
DOI: 10.1177/1077546314532119
jvc.sagepub.com


Abstract

The dynamic stability of a coupled tower-blade wind turbine system is investigated analytically and experimentally. Coupled equations of motion and associated boundary conditions for the wind tower and a rotating blade are derived by considering the lateral acceleration of the nacelle at the tip of the tower, which is the base of the flexible blade. The coupled eigenvalues are computed for various blade rotational speeds and densities of the tower material by using Galerkin's method in spatial coordinates. The results indicate that the coupled tower-blade system becomes unstable when certain vibrational modes of the tower and blade coalesce. Additionally, the vibration of the rotating blades is measured using a wireless telemetry system attached to the small-scale tower-blade wind power system, and the results are compared with those of the analytical study. The experiment shows that instability is observed in the same ranges of the blade rotational speed as those predicted by our analytical study.

Keywords

Coupled tower-blade system, eigenvalue veering, mode coalescence, stability, wind turbine system

1. Introduction

Ever since the Kyoto Protocol came into effect in 2005, several countries have expanded their efforts to reduce greenhouse gas emissions. Wind, being one of the renewable energy sources, presents the possibility of generating pollution-free power. Recently, Johnson et al. (2013) reported that wind power generation requires fewer resources than coal-based or solar power generation. Moreover, the construction of larger-sized wind power generators has reduced the cost of operations and maintenance, and facilitated improvements in the efficiency and volume of power generation (Manwell et al., 2003). However, the breakage of a blade or the tower in the system may cause disasters (Ciang et al., 2008); hence, in order to prevent failure, it is necessary to analyze the dynamic characteristics of a wind power system accurately and well in advance.

Among the main components of a wind generator, the highest proportions of manufacturing costs are accounted for by the tower (26.3%) and rotor blades (22.2%) (Crispin, 2007). The rotor blades convert wind

energy into rotary power. Blades must have an optimal design because the aerodynamic and dynamic forces caused by rotation significantly affect the performance of a wind generator. Because the blade harnesses wind power when being rotated at an altitude of several hundred feet, it is directly exposed to wind loads and subjected to bending and torsional stresses simultaneously. These loading conditions are repeatedly sustained and depending on the wind strength, can induce vibration leading to fatigue and in turn, cracking and breakage over time. The Caithness Windfarm Information

¹School of Mechanical Engineering, Kyungpook National University, Daegu, Korea

²R&D Center, Korea Powertrain Co. Ltd., Daegu, Korea

³School of Mechanical Engineering, Hanyang University, Seoul, Korea

⁴Department of Mechanical and Aerospace Engineering, University of California, Irvine, USA

Received: 23 December 2013; accepted: 15 March 2014

Corresponding author:

Namcheol Kang, School of Mechanical Engineering, Kyungpook National University, 1370 Sankyuk-dong, Buk-gu, Daegu, Korea.
Email: nckang@knu.ac.kr

Forum (2013) has reported that blade damage occurs most frequently in wind generator parts, and blade debris can fall as far as one mile away.

Although many studies have been conducted on rotating blades because of their similarity to conventional engineering devices such as turbine blades or helicopter rotary wings (Hoa, 1979; Bhat, 1986; Yoo and Shin, 1998), relatively fewer studies are available on the effects of coupling in tower-blade systems. Garrad and Quarton (1986) derived a model for the coupled tower-rotor system of a wind turbine by using symbolic computing techniques, and performed stability analysis on a simple example. As they did not include the nacelle and considered only the tower and blades, the example was physically closer to a helicopter. Furthermore, Chen et al. (2009) analyzed the wind-induced response of a wind turbine tower and obtained computational results on the influence of the tower-blade coupling effect on a wind turbine system. They found that the total base shear of the blades can increase the maximal displacement by approximately 300%. Recently, Kessentini et al. (2010) developed a mathematical model of the 1HAWT with flexible tower and blades by considering the nacelle pitch angle and structural damping. They examined the effects of pitch angle and blade orientation on natural frequencies. By studying the time response, they concluded that small amplitudes of tower motion may induce relatively larger amplitudes of blade motion.

Several studies have reported the coupling effect using interactive boundary conditions that separately influence the tower or blades. Burton et al. (2001) interpreted blade movement characteristics by considering the motion of the top part of the tower due to the dynamic forces acting on the blade. Moreover, Murtagh et al. (2005) analyzed the tower-blade coupling effect, considering the shear forces generated at the end of the tower owing to blade rotation. They numerically solved the equation of motion for tower vibrations, including the blade shear forces as the forcing function. They further investigated the effect of the tuned mass damper (TMD) on wind turbine vibrations (Murtagh et al., 2008) using their previously developed coupled tower-blade analytical model. Hau (2006) emphasized that the first and foremost requirement of the wind turbine from the vibration perspective is preventing the exciting rotor forces from resonating with the tower bending mode. Recently, Liu (2013) analyzed the blade-cabin-tower coupling system of the wind turbine to calculate the natural frequency of the tower based on the kinetic equation of the simplified single-degree-of-freedom tower model, and ultimately

evaluated the total wind force in the system. However, the limitation of these studies is that they did not consider the mutual coupling between the tower and rotating blade, but one directional influence to the other.

In contrast, when Larsen and Nielsen (2006) investigated the nonlinear coupled dynamics of wind turbine wings, they considered the interaction between the nacelle and wings as the motion of the wing supports caused by the stationary motion of the turbine. Furthermore, they performed nonlinear parametric stability analysis of the wind turbine wings, assuming harmonically varying support point motions from the tower (Larsen and Nielsen, 2007) and found that the wind turbine system becomes unstable at certain excitation amplitudes and frequencies. However, they considered the coupling effect as the decoupling of the wing from the nacelle and the tower, by introducing translation and rotation.

Additionally, there have been several attempts to use mixed flexible rigid-body models for modeling the coupled tower-blade systems. Lee et al. (2002) performed structural dynamic analysis representing the wind turbine as a multiflexible body system with both rigid-body (nacelle, hub) and flexible-body (blades, tower) subsystems. The governing coupled equations were linearized about the steady-state solution after which Floquet theory was used to obtain the characteristics of the entire system. Similarly, Wang et al. (2010) analyzed the coupled dynamic performances of a wind turbine system by deriving a mixed flexible-rigid, multi-body mathematical model and used it to study the influence of tower stiffness on blade tip deformation. Additionally, he demonstrated that the dynamic displacement of the blades is influenced considerably by that of the tower, but he did not perform further stability analysis. Recently, Staino and Basu (2013) proposed the modeling and control of vibrations in wind turbines at different blade rotational speeds. Using a Lagrangian approach, they formulated a multimodal model for representing the dynamics of the blades and their interaction with the tower. However, they used a single-degree-of-freedom model for the tower and nacelle with modal mass.

It is well known that the stability of a system is generally analyzed using either forced or free vibration (or eigenvalue) analyses. The first approach is useful when the external forcing functions are well defined, whereas the second is more applicable when unknown forces are involved; it is more useful for understanding the interactions of the vibration modes. Because the external forces (due to wind or earthquake) on a wind turbine system are usually unpredictable, we adopted the

eigenvalue analysis approach to investigate the instability mechanism caused by the rotating blade and tower vibration modes. In general, when the natural frequencies of several structures are close to each other, their dynamic behaviors are coupled, and interaction occurs. Thus, for analyzing the dynamic characteristics of coupled structures, identifying the specific characteristics, determining the design factors through coupled analysis, and deriving the coupled equations of motion of the entire system are necessary. Moreover, if the signals measured in the structures are compared and analyzed, the onset of damage can be detected in advance using the computational results of the coupled analysis, and damage can be prevented.

In this study, eigenvalue analysis of a coupled tower-blade system was performed by considering the interaction between the motion of the nacelle and the rotating blades. The coupled equations of motion and associated boundary conditions were derived and the coupled natural frequencies were calculated by applying Galerkin's method in space. Additionally, a small-scale prototype of a coupled tower-blade wind power system was built and experiments were conducted using a wireless telemetry measurement system that recorded the vibrations of the rotating blades. Finally, the experimental results were seen to be in good agreement with the analytical results.

2. Analytical study

The classical equations of motion describing the small-amplitude transverse vibrations of the tower and rotating blades were used for conducting the coupled analysis of the tower-blade wind turbine system. Furthermore, the interaction between the tower and blades was explained by considering the force equilibrium conditions at the nacelle. Applying Galerkin's method in spatial coordinates, we obtained discretized equations for the coupled tower-blade system. The eigenvalue analysis was performed using the blade rotating speed and tower material density as variables.

2.1. Mathematical modeling of coupled tower-blade system

Figure 1 shows a coupled tower-blade wind power system, in which a point mass M_0 of the nacelle is attached to the tip of the tower, with a blade rotating at speed Ω . Both the tower and blade are assumed to be Bernoulli-Euler beams with homogeneous and uniform cross sections. The symbols ρ , A , E , and I represent the density per unit volume, cross-sectional area, Young's

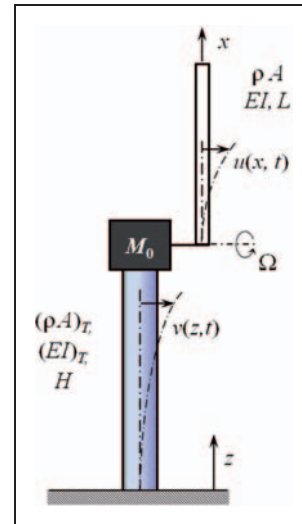


Figure 1. Simplified coupled tower-blade model.

modulus, and moment of inertia of the cross section, respectively. The subscript T represents the tower. A simplified two-dimensional model is considered wherein deformation of the tower and blade occurs in the same plane. Two variables, z and x , are used to denote the local spatial coordinates of the tower and blade along the length, respectively. Additionally, the out-of-plane transverse vibrations of the tower and blade are described as $v(z, t)$ and $u(x, t)$, respectively.

Neglecting the axial force due to the weights of the nacelle/blade or the lateral force due to wind/earthquake, the equation of motion governing the transverse displacement of the tower (Meirovitch, 2000) is expressed as

$$(\rho A)_T \frac{\partial^2 v(z, t)}{\partial t^2} + (E I)_T \frac{\partial^4 v(z, t)}{\partial z^4} = 0 \quad (1)$$

It is assumed that the tower is fixed to the ground and the nacelle with the rotating blade is located at the other end of the tower. Considering the tower separately from the blade, the former's end-tip is subjected to the interactive forces caused by the motion of the nacelle and the blade. The interactive force caused by the nacelle is proportional to its mass and acceleration, which is equal to the temporal second derivatives of the deflection of the tower's end-tip. Moreover, the interactive force due to the rigid-body motion and the vibrations of the rotating blades is additionally transmitted to the tower (Hansen, 2008). These forces can be considered as shear forces using the boundary condition acting on the end-tip of the tower. On the other

hand, the moment on this end-tip is neglected because the change in the rotational angle of the nacelle due to the vibration of the blade is small. By applying the force equilibrium condition in the horizontal direction, as shown in Figure 2, the associated boundary conditions for transverse vibrations of the tower can be obtained as follows:

Displacement:

$$v(z, t)|_{z=0} = 0 \quad (2)$$

Slope:

$$\frac{\partial v(z, t)}{\partial z} \Big|_{z=0} = 0 \quad (3)$$

Moment:

$$(EI)_T \frac{\partial^2 v(z, t)}{\partial z^2} \Big|_{z=H} = 0 \quad (4)$$

Shear force:

$$\left[\frac{\partial}{\partial z} \left((EI)_T \frac{\partial^2 v(z, t)}{\partial z^2} \right) \right]_{z=H} = (M_0 + \rho AL) \frac{\partial^2 v(z, t)}{\partial t^2} \Big|_{z=H} + \int_0^L \rho A \frac{\partial^2 u(x, t)}{\partial t^2} dx \quad (5)$$

The transverse vibration of the rotating blade is also governed by the Bernoulli-Euler beam equation. However, the blade is subjected not only to centrifugal forces due to its own rotation but also transverse motion of the base due to the vibration of the tower, because the blades are clamped on the nacelle, which, in

turn, is fixed to the end-tip of the tower. Therefore, the total blade displacement (Chopra, 1995) is

$$u^{total}(x, t) = u(x, t) + v(z, t)|_{z=H} \quad (6)$$

where the blade displacement $u(x, t)$ is defined relative to the support motion $v(z, t)|_{z=H}$. Recognizing that the inertia forces of the blade are related to the total acceleration values, we obtain the governing equation for the rotating blade using the base excitation caused by tower vibration and the centrifugal force due to blade rotation, and is given as

$$\rho A \left[\frac{\partial^2 u(x, t)}{\partial t^2} + \frac{\partial^2 v(z, t)}{\partial t^2} \Big|_{z=H} \right] + EI \frac{\partial^4 u(x, t)}{\partial x^4} - \frac{\partial}{\partial x} \left[F_c(x) \frac{\partial u(x, t)}{\partial x} \right] = 0 \quad (7)$$

where $F_c(x)$ indicates the centrifugal force in the blade due to its own rotation. Using the dummy variable s , this force can be calculated as follows (Meirovitch, 2000):

$$F_c(x) = \int_x^L \rho A s \Omega^2 ds \quad (8)$$

The clamped and free boundary conditions for the rotating blade are given as follows:

Displacement:

$$u(x, t)|_{x=0} = 0 \quad (9)$$

Slope:

$$\frac{\partial u(x, t)}{\partial x} \Big|_{x=0} = 0 \quad (10)$$

Moment:

$$EI \frac{\partial^2 u(x, t)}{\partial x^2} \Big|_{x=L} = 0 \quad (11)$$

Shear force:

$$EI \frac{\partial^3 u(x, t)}{\partial x^3} \Big|_{x=L} = 0 \quad (12)$$

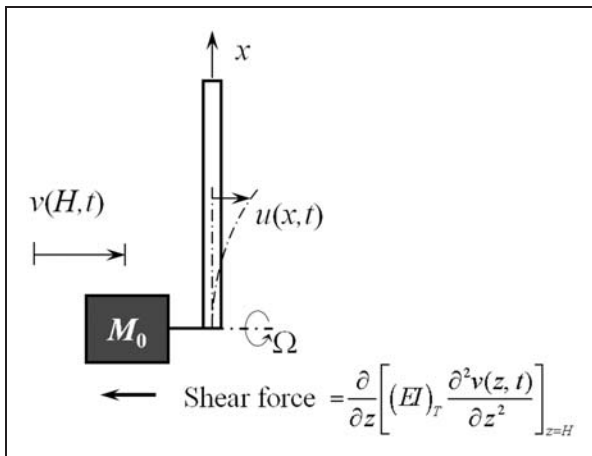


Figure 2. Free-body diagram of nacelle and rotating blade.

Recalling the total displacement of the blade in equation (6), the essential (or geometric) boundary conditions for the blade at $x=0$ are identical to those of the tower at $z=H$.

As previously derived, the motions of the tower and rotating blade are coupled by means of the interactive forces on the tower due to the nacelle and the base motion of the blade, included in the governing equations. This implies that the boundary condition of the tower is determined by the shear forces due to the nacelle and rotating blade (equation (5)), and the blade motion is subjected to the base motion caused by tower vibration, as described in equation (7). Therefore, investigating the dynamic behavior of the coupled tower-blade system requires solutions to be found that satisfy the governing equations (equations (1) and (7)) and the corresponding boundary conditions given by equations (2)–(5) and (9)–(12).

2.2. Eigenvalue analysis using Galerkin's method in spatial coordinates

Galerkin's method was used to find the eigenvalues of the coupled tower-blade system. Assuming harmonic motions of their vibrations, the transverse displacements of the tower and blade are, respectively, given by

$$v(z, t) = V(z)e^{-i\omega t}, \quad u(x, t) = U(x)e^{-i\omega t} \quad (13)$$

where i and ω indicate $\sqrt{-1}$ and frequencies, respectively. Applying the separation of the variables method to the tower's equation of motion (equation (1)), we obtain the fourth-order ordinary differential equation with respect to the spatial variable z as follows:

$$(EI)_T \frac{d^4 V(z)}{dz^4} - \omega^2 (\rho A)_T V(z) = 0 \quad (14)$$

From equations (2)–(5), the associated boundary conditions are obtained as follows:

$$V(0) = \frac{dV(z)}{dz} \Big|_{z=0} = \frac{d^2 V(z)}{dz^2} \Big|_{z=H} = 0 \quad (15)$$

$$\left[\frac{d}{dz} \left((EI)_T \frac{d^2 V(z)}{dz^2} \right) \right]_{z=H} = -\omega^2 \left[(M_0 + \rho AL)V(H) + \int_0^L \rho AU(x)dx \right] \quad (16)$$

Similarly, the equation of motion (equation (7)) and the boundary conditions (equations (9)–(12)) for the rotating blade are transformed as follows:

$$-\omega^2 \rho AU(x) + EI \frac{d^4 U(x)}{dx^4} - \frac{d}{dx} \left[F_c(x) \frac{dU(x)}{dx} \right] = \omega^2 \rho AV(H) \quad (17)$$

$$U(x) \Big|_{x=0} = \frac{dU(x)}{dx} \Big|_{x=0} = \frac{d^2 U(x)}{dx^2} \Big|_{x=L} = \frac{d^3 U(x)}{dx^3} \Big|_{x=L} = 0 \quad (18)$$

To investigate the characteristics of the coupled tower-blade system by applying Galerkin's method to solve the ordinary differential equations in z and x , the displacements of the blade and tower, $U(x)$ and $V(z)$, were assumed, respectively, to be

$$U(x) = \sum_{j=1}^N a_j \phi_j(x), \quad V(z) = \sum_{j=1}^M b_j \psi_j(z) \quad (19)$$

where a_j and b_j are undetermined coefficients, and N and M are the number of series terms in the blade and tower deformation modes, respectively. The terms $\phi_j(x)$ and $\psi_j(z)$ are admissible functions satisfying the essential boundary conditions, which are given as:

$$\phi_j(x) = 1 - \cos \left[\frac{(2j-1)\pi x}{2L} \right] \quad (20)$$

$$\psi_j(z) = 1 - \cos \left[\frac{(2j-1)\pi z}{2H} \right] \quad (21)$$

Substituting equation (19) into equations (14) and (17), and applying Galerkin's method along with the boundary conditions, the discretized coupled matrix equations are obtained.

$$\begin{bmatrix} (\mathbf{K}_{11})_{ij} & 0 \\ 0 & (\mathbf{K}_{22})_{ij} \end{bmatrix} \begin{Bmatrix} a_i \\ b_j \end{Bmatrix} - \omega^2 \begin{bmatrix} (\mathbf{M}_{11})_{ij} & (\mathbf{M}_{12})_{ij} \\ (\mathbf{M}_{21})_{ij} & (\mathbf{M}_{22})_{ij} \end{bmatrix} \begin{Bmatrix} a_i \\ b_j \end{Bmatrix} = 0 \quad (22)$$

where

$$(\mathbf{K}_{11})_{ij} = \int_0^L EI \phi_i''(x) \phi_j''(x) dx + \frac{1}{2} \int_0^L \rho A \Omega^2 (L^2 - x^2) \phi_i'(x) \phi_j'(x) dx \quad (23)$$

$$(\mathbf{K}_{22})_{ij} = \int_0^H (EI)_T \psi_i''(z) \psi_j''(z) dz \quad (24)$$

$$(\mathbf{M}_{11})_{ij} = \int_0^L \rho A \phi_i(x) \phi_j(x) dx \quad (25)$$

$$(\mathbf{M}_{12})_{ij} = \int_0^L \rho A \phi_i(x) \psi_j(H) dx \quad (26)$$

$$(\mathbf{M}_{21})_{ij} = \int_0^L \rho A \psi_i(H) \phi_j(x) dx \quad (27)$$

$$(\mathbf{M}_{22})_{ij} = (M_0 + \rho A L) \psi_i(H) \psi_j(H) + \int_0^H (\rho A)_T \psi_i(z) \psi_j(z) dz \quad (28)$$

All sub-matrices in this matrix equation are apparently symmetric except the off-diagonal terms $(\mathbf{M}_{12})_{ij}$ and $(\mathbf{M}_{21})_{ij}$. Furthermore, $(\mathbf{M}_{12})_{ij}$ and $(\mathbf{M}_{21})_{ij}$ are transposes of each other because $\psi_j(H)$ is always the unity recalling equation (equation (21)). The coupled system is now well posed, and hence, a simple eigenvalue solver such as a quotient reduction (QR) algorithm can be used to obtain convergent solutions. The eigenvalues of the coupled tower-blade system were calculated with the condition that the determinant of equation (22) vanishes, to obtain non-zero solutions.

2.3. Stability of coupled tower-blade system

The eigenvalue analysis of the coupled tower-blade wind turbine system was performed using the specifications listed in Table 1. The materials of the tower and blade were assumed to be steel and aluminum, respectively, and the nacelle was considered to be a point mass. Through an in-depth study, we found that N and M in equation (19) show good convergence at 30. The natural frequencies of the uncoupled and coupled tower-blade systems with respect to the blade rotating speed were determined using MATLAB. The natural

Table 1. Specifications of wind power system used in computation.

Part	Property	Dimension
Tower (steel)	Height (H)	46 m
	Inner radius	1.5 m
	Outer radius	1.49 m
	Density (ρ_t)	7850 kg/m ³
	Young's modulus (E_t)	210 GPa
Blade (aluminum)	Length (L)	22 m
	Width	0.5 m
	Thickness	0.1 m
	Thickness density (ρ)	2770 kg/m ³
	Young's modulus (E)	69 GPa
Nacelle	Mass (M_0)	30,000 kg

frequencies calculated from the real and imaginary parts of the eigenvalues are plotted in the upper and lower parts of Figure 3, respectively. The dashed and solid lines indicate uncoupled and coupled natural frequencies of the tower-blade system, respectively. Mode numbers are also identified and indicated in the figure based on our eigenvalue analysis of the uncoupled system. For example, the first and second uncoupled vibration modes of the tower are denoted as 1T and 2T, respectively, and the blade modes as 1B, 2B. *It should be noted that in the uncoupled system, whereas the natural frequencies of the blade increase owing to the stiffening effect caused by the increase in blade rotating speed, those of the tower remain constant (Figure 3). In contrast, in the coupled system, the natural frequencies show more complicated trends.*

In particular, the coupled tower-blade system becomes unstable for a certain range of rotating speeds. When the imaginary parts of the eigenvalues are positive at approximately 75–100 RPM, the responses become unbounded (as per equation (13)).

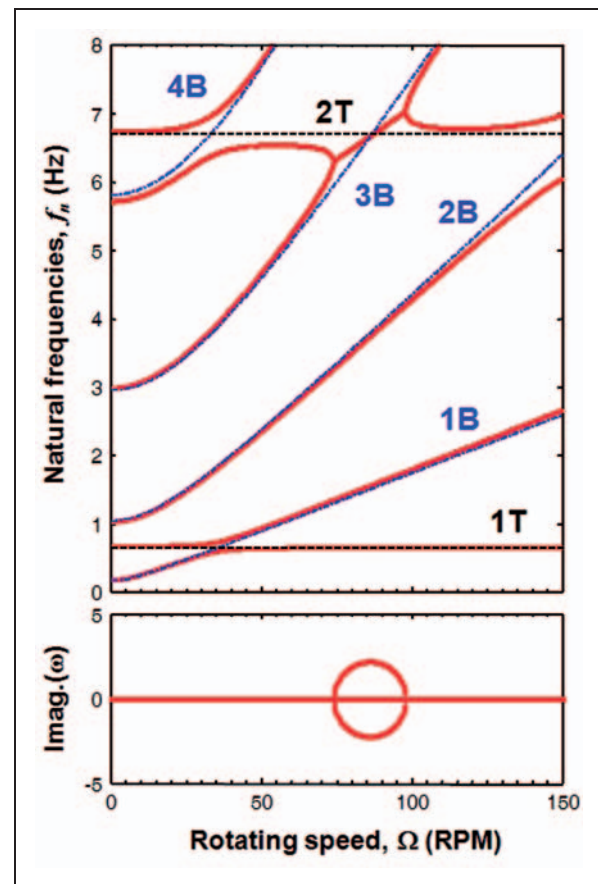


Figure 3. Natural frequencies of coupled and uncoupled tower-blade systems when blade rotates from 0 to 150 RPM (dashed line: uncoupled tower mode; dashed-dotted line: uncoupled blade mode; solid line: coupled tower-blade mode).

Instability occurs when tower and blade modes coalesce, i.e., in the range in which the second tower mode coalesces with the third blade mode. Conversely, when the first tower mode approaches the second blade mode, mode coalescence does not occur. However, the eigenvalue veering phenomenon occurs and the system remains stable. Interestingly, similar instability mechanisms exist in the rotating disk in an enclosed compressible fluid (Kang and Raman, 2004). From our in-depth investigations of the higher modes, two coupling rules can be generalized: first, whenever an odd or even tower mode approaches an even or odd blade mode, respectively, mode coalescence occurs, causing the coupled tower-blade system to become unstable for a certain range of rotating speeds; and second, when an odd or even tower mode approaches an odd or even blade mode, respectively, eigenvalue veering occurs but the coupled tower-blade system remains stable during that time.

A parametric study of the eigenvalue analysis was also performed for varying densities of the tower material. Figure 4 illustrates the natural frequencies of

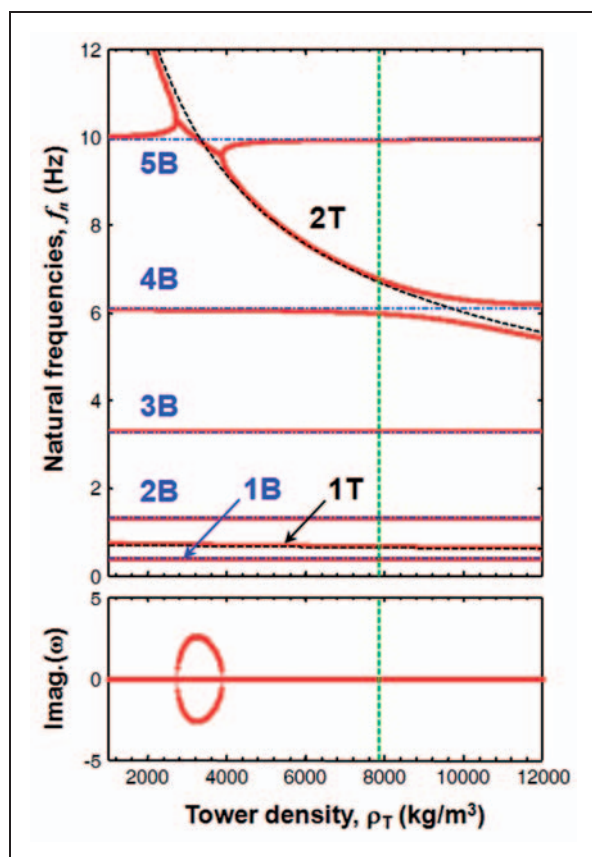


Figure 4. Natural frequencies of coupled and uncoupled tower-blade systems when tower material density varies from 1000 to 12000 kg/m³ at 20 RPM (dashed line: uncoupled tower mode; dashed-dotted line: uncoupled blade mode; solid line: coupled tower-blade mode; dashed green line: tower material density at base model).

coupled and uncoupled tower-blade systems at an example rotating speed of 20 RPM, with the tower material density varying from 1000 to 12,000 kg/m³. Dashed and solid lines indicate the natural frequencies of the uncoupled and coupled tower-blade systems, respectively. In the former, the natural frequencies of the blade are constant with the increase in tower material density whereas those of the tower decrease owing to increasing mass effect. To compare this with the previous results, the base model in which the tower material density is 7850 kg/m³ is also depicted as a dashed vertical green line. The base model, which is a coupled system, shows a stable operating condition, but the coupled eigenvalues veer slightly at this rotating speed. However, the model experiences an unstable condition when the second tower mode coalesces with the fifth blade mode. This instability occurs when the density of the tower material (aluminum) is 2400–4000 kg/m³. Excessive reduction in the tower material density for saving material costs or other reasons can cause serious stability problems. The computational results demonstrate that the analysis of the coupling between the tower and rotating blade is instructive to understand the modal interactive mechanism of the instability and is significant for the avoidance of unstable operating conditions or structural instability in the wind turbine system.

3. Experimental investigation

The flapwise vibrations of the rotating blades of a small-scale prototype of the tower-blade system were measured, and the results were compared with the computational results.

3.1. Small-scale prototype of wind turbine

A small-scale prototype of the wind turbine was built in our laboratory to investigate the dynamic characteristics of the coupled tower-blade system. Heavy steel was used to build the tower to support the weight of the nacelle and withstand the centrifugal forces exerted by the rotating blade. For easy operation, the height and hollow cross-sectional thickness of the tower were designed to be 1 m and 3 mm, respectively. Considering the ratio of the blade length to the tower height to be half of that of the J48/750 commercial wind power system, the length of the rotating blade in the small-scale prototype was set to 0.5 m. The detailed specifications of the small-scale prototype are listed in Table 2.

Although rotating blades are generally made of composite materials and with a complex shape in an actual wind turbine, an aluminum blade with rectangular cross section was used for the purpose of comparison with computational results. Moreover, our small-scale

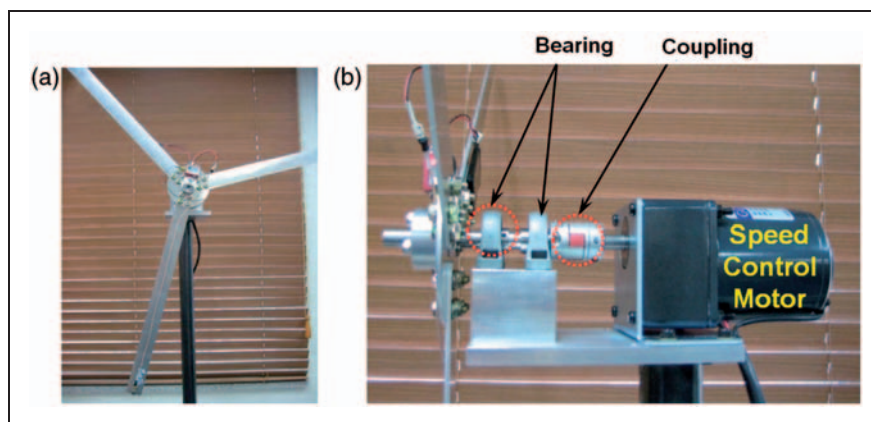
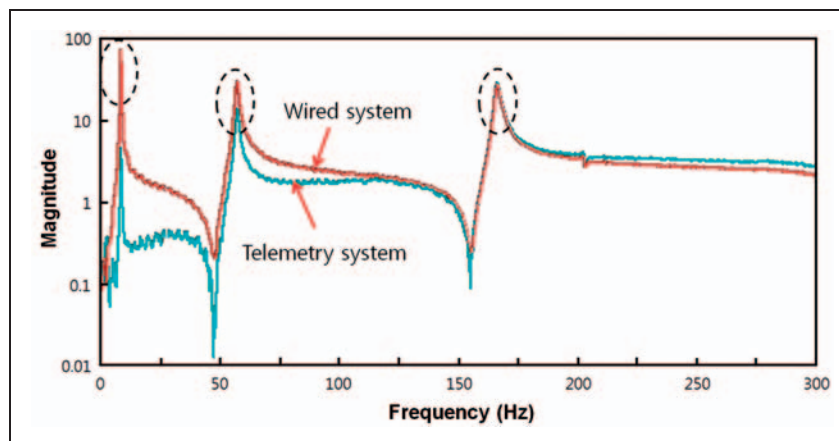
Table 2. Specifications of small-scale coupled tower-blade system.

Part	Property	Dimension
Tower (steel)	Height (H)	1.0 m
	Outer radius	21 mm
	Inner radius	18 mm
	Density (ρ_t)	7850 kg/m ³
	Young's modulus (E_t)	210 GPa
Blade (aluminum)	Length (L)	0.51 m
	Width	40 mm
	Thickness	3 mm
	Thickness density (ρ)	2700 kg/m ³
	Young's modulus (E)	69 GPa
Nacelle	Mass (M_0)	3.95 kg

indoor prototype uses an electric motor in the nacelle with rotating speed in the range 0–500 RPM, although a real wind turbine uses the surrounding airflow. Finally, to minimize damage or unwanted disturbances from the motor, the bearing and coupling were connected between the motor and blade, as shown in Figure 5.

3.2. Comparisons between wired and wireless telemetry systems

First, to validate the wireless telemetry measurement system used in the rotating blade, the results of the experiment were compared with those of a non-rotating blade. The accelerations of a 0.5-m-long and 3-mm-thick uniform aluminum blade were measured using wired and wireless telemetry systems simultaneously.

**Figure 5.** Small-scale prototype of coupled tower-blade wind turbine system. (a) front view (b) side view.**Figure 6.** Frequency response functions of cantilever beam for comparing spectral properties using wired and wireless telemetry systems.

For a clamp-free blade, hammering tests were performed and frequency response functions were obtained using the commercial software eZ-analyst (IOtech, 2006).

We confirmed that the spectral properties of the wired and wireless telemetry systems were identical, as shown in Figure 6. Because the natural frequencies of the cantilever beam measured by the wireless and wired telemetry systems were the same, we concluded that the former was capable of satisfactorily measuring the vibration of the rotating blade. However, we also found that the magnitudes of the vibration modes are slightly different across wired and wireless systems owing to insufficient sensitivity of the latter under a frequency of 50 Hz. Nevertheless, it is reasonable to assume that the wireless system is acceptable because instability generally occurs at a frequency higher than 50 Hz and stability characteristics are based mainly on the loci of the natural frequencies. Thus, the wireless telemetry system was selected for measuring rotating blade vibrations in this study.

3.3. Experimental results for rotating tower-blade system

In the absence of external forces, the flapwise bending vibrations of the rotating blade were measured in the small-scale prototype of the wind turbine, as illustrated in Figure 7. An accelerometer (type 4807, B&K) was attached to the end-tips of the rotating blade and the measured signals were transferred to a transmitter fixed on the rotating hub (Figure 8). Via radio

frequency, the signals were transferred to the receiver and analyzed using data acquisition and analog-to-digital converting processes. Table 3 lists the detailed specifications of the wireless telemetry system. The measurements were repeated 20 times according to a linear averaging scheme to minimize the effect of noises. The measured signals were spectrally analyzed using eZ-analyst.

Both the computational and experimental natural frequencies are plotted in Figure 9 with respect to the

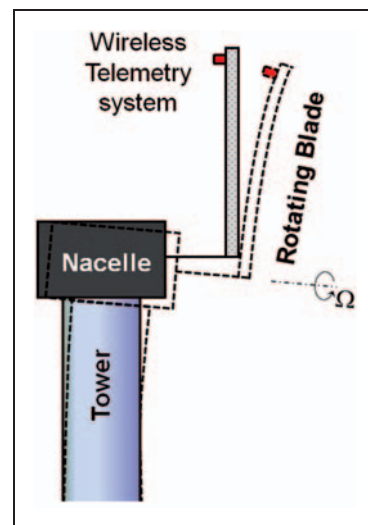


Figure 7. Configuration of measurement locations for accelerometers for measuring vibrations of tower and rotating blade.

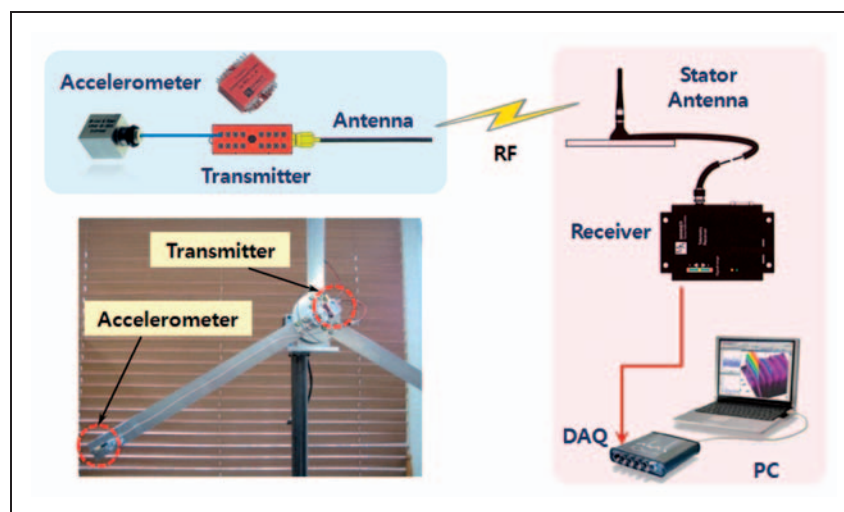


Figure 8. Configuration of wireless telemetry measurement system.

blade rotating speed in the steady-state condition. For easy comparison with the analytical results, the natural frequencies (computed using Galerkin's method for the small-scale prototype) are plotted in Figure 9(a). As described in subsection 2.3, the coupled tower-blade prototype became unstable at approximately 350 RPM owing to coalescence of the second tower mode with the third blade mode. The auto power spectrum of the flapwise acceleration at the tip of the rotating blade is plotted in Figure 9(b), in which red and blue colors indicate high and low amplitudes of acceleration,

respectively. Detecting the first tower and blade modes in the low frequency region was not possible owing to poor signal-to-noise ratio. However, similar to the computational results, the second mode of the rotating blade appeared at approximately 60 Hz at 0 RPM and increased with an increase in the rotating speed. Additionally, the second tower and third blade modes were measured in slightly lower frequency ranges than those of the computational cases, and frequency increase due to the stiffening effect caused by the centrifugal force was also observed. In particular, the amplitude of blade vibration dramatically increased from approximately 350 RPM to 500 RPM, and these ranges agreed well with those predicted analytically. In the experiment, the vibration modes may be measured at slightly lower frequencies than those of the computational cases because of the added mass effect due to the attachment of the accelerometer and the transmitter of the telemetry system. Furthermore, the acceleration of the actual system is limited owing to damping caused by the bolts between the tower and blades, bearings, couplings, etc., whereas that of the theoretically undamped system is unlimited in unstable regions. Therefore, in the future, it would be more practical to include the effects of multiblades and damping on the dynamic stability of the wind power system.

Table 3. Specifications of wireless telemetry system.

Component	Specification
Transmitter	Bandwidth: 0–1 kHz Sample rate: 3.75 kHz Size: 36 × 34 × 13 mm Mass: 12 g
Receiver	Bandwidth: 0–1 kHz RF frequency: 433 MHz
Antenna	Size: 150 × 101 × 35.5 mm RF frequency: 433 MHz Height: 87 mm

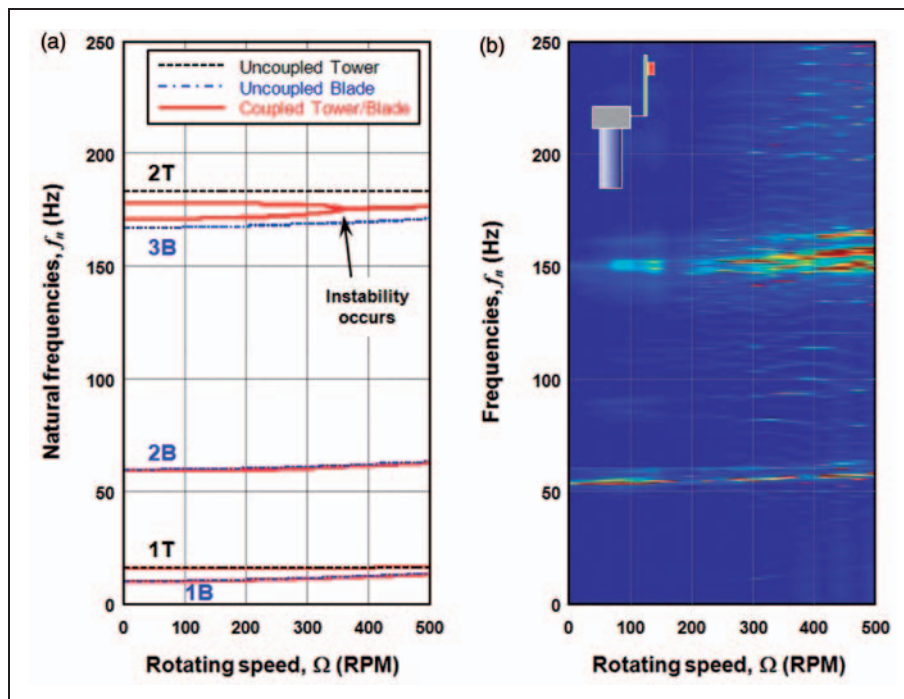


Figure 9. Computational and experimental natural frequencies of coupled tower-blade system. (a) computational results (b) blade acceleration results from experiment.

4. Conclusions

We investigated the dynamic characteristics of a coupled tower-blade wind turbine analytically and experimentally. Coupled equations of motion with boundary conditions were derived by considering the interaction between the motion of the tower and rotating blades. Eigenvalues were computed and stability analysis was performed by applying Galerkin's method in spatial coordinates for various blade rotating speeds and tower material densities. Based on the computational results, we found that either eigenvalue veering or mode coalescence occurred when the tower and rotating blade vibration modes approached each other. Depending on the mode numbers of the tower and blades, different coupling rules were established, and we found that the coupled system became unstable during mode coalescence. Additionally, experimental investigations of the coupled system were performed using a wireless telemetry system attached to a small-scale prototype wind turbine system. Through spectral analysis, instability was observed in the experimental studies at the same ranges of rotating speeds as those in the present analytical study. Based on the comparison between our analytical and experimental results for the coupled tower-blade system, we confirmed the validity of the instability mechanism observed in our study.

Funding

This work was supported by the Basic Science Research Program through the National Research Foundation of Korea (NRF), funded by the Ministry of Education, Science and Technology (grant number 2010-0006654).

References

- Bhat RB (1986) Transverse vibrations of a rotating uniform cantilever beam with tip mass as predicted by using beam characteristic orthogonal polynomials in the Rayleigh-Ritz method. *Journal of Sound and Vibration* 105: 199–210.
- Burton T, Sharpe D, Jenkins N and Bossanyi E (2001) *Wind Energy Handbook*. Chichester, England: John Wiley & Sons Ltd.
- Caithness Windfarm Information Forum (2013) Summary of wind turbine accident data to 30 September 2013. Available at: <http://www.caithnesswindfarms.co.uk/page4.htm> (accessed 23 December 2013).
- Chen X, Li J and Chen J (2009) Wind-induced response analysis of a wind turbine tower including the blade-tower coupling effect. *Journal of Zhejiang University-Science A* 10(11): 1573–1580.
- Chopra AK (1995) *Dynamics of Structures*. New Jersey: Prentice-Hall, Inc.
- Ciang CC, Lee JR and Bang HJ (2008) Structural health monitoring for a wind turbine system: a review of damage detection methods. *Measurement Science and Technology* 19: 122001.
- Crispin A (2007) Focus on supply chain. *Wind Directions*, January/February. European Wind Energy Association.
- Garrad AD and Quarton DC (1986) Symbolic computing as a tool in wind turbine dynamics. *Journal of Sound and Vibration* 109(1): 65–78.
- Hansen MOL (2008) *Aerodynamics of Wind Turbines*. London: Earthscan.
- Hau E (2006) *Wind Turbines: Fundamentals, Technologies, Application, Economics*. Berlin: Springer-Verlag.
- Hoang SV (1979) Vibration of a rotating beam with tip mass. *Journal of Sound and Vibration* 67: 369–381.
- IOtech (2006) eZ-Analyst user's manual. Available at: www.ni.com/pdf/products/us/ez_analyst.pdf (accessed 23 December 2013).
- Johnson LT, Yeh S and Hope C (2013) The social cost of carbon: implications for modernizing our electricity system. *Journal of Environmental Studies and Sciences* 3: 369–375.
- Kang N and Raman A (2004) Aeroelastic flutter mechanisms of a flexible disk rotating in an enclosed compressible fluid. *Journal of Applied Mechanics* 71: 120–131.
- Kessentini S, Choura S, Najjar F and Franchek MA (2010) Modeling and dynamics of a horizontal axis wind turbine. *Journal of Vibration and Control* 16(13): 2001–2021.
- Larsen JW and Nielsen SRK (2006) Non-linear dynamics of wind turbine wings. *International Journal of Non-Linear Mechanics* 41: 629–643.
- Larsen JW and Nielsen SRK (2007) Nonlinear parametric instability of wind turbine wings. *Journal of Sound and Vibration* 299: 64–82.
- Lee D, Hodges DH and Patil MJ (2002) Multi-flexible-body dynamic analysis of horizontal axis wind turbines. *Wind Energy* 5: 281–300.
- Liu WY (2013) The vibration analysis of wind turbine blade-cabin-tower coupling system. *Engineering Structures* 56: 954–957.
- Manwell JF, McGowan JG and Rogers AL (2003) *Wind Energy Explained*. New York: John Wiley & Sons Ltd.
- Meirovitch L (2000) *Fundamentals of Vibrations*. New York: McGraw-Hill Companies Inc.
- Murtagh PJ, Basu B and Broderick BM (2005) Along-wind response of a wind turbine tower with blade coupling subjected to rotationally sampled wind loading. *Engineering Structures* 27: 1209–1219.
- Murtagh PJ, Ghosh A, Basu B and Broderick BM (2008) Passive control of wind turbine vibrations including blade/tower interaction and rotationally sampled turbulence. *Wind Energy* 11: 305–317.
- Staino A and Basu B (2013) Dynamics and control of vibrations in wind turbines with variable rotor speed. *Engineering Structures* 56: 58–67.
- Wang J, Qin D and Lim TC (2010) Dynamic analysis of horizontal axis wind turbine by thin-walled beam theory. *Journal of Sound and Vibration* 329: 3565–3586.
- Yoo HH and Shin SH (1998) Vibration analysis of rotating cantilever beams. *Journal of Sound and Vibration* 212: 807–828.